

Load and response quantification of direct fixation fastening systems for heavy rail transit infrastructure

Proc IMechE Part F:
J Rail and Rapid Transit
2021, Vol. 235(9) 1110–1121
© IMechE 2021
Article reuse guidelines:
sagepub.com/journals-permissions
DOI: 10.1177/0954409720987036
journals.sagepub.com/home/pif



Arthur de O Lima¹ , J Riley Edwards¹ ,
Luis W Chavez Quiroz² , Yu Qian³ and Marcus S Dersch¹

Abstract

Ballastless track (i.e. slab track) systems are used extensively in passenger rail applications for improved track stability, alignment control, vibration, and life cycle cost (LCC) benefits. These systems regularly rely on Direct Fixation (DF) fasteners to connect the rail to the structure. Field performance observations have indicated that even under similar track geometry and train operating conditions, the DF fasteners useful life varies widely. Meanwhile, a review of literature reveals that there is limited prior research to guide optimization of DF fastener designs for heavy rail transit. Therefore, researchers at the University of Illinois at Urbana-Champaign (UIUC) conducted a field investigation at three sites on a United States legacy heavy rail transit system to quantify wheel-rail interface loading demands and DF fastener response. Track response variance across similar track geometry was found. Wheel loads ranged between 2.7 to 18.2 kip (12.0 to 81.0 kN) and 0.9 to 12.4 kip (4.0 to 55.2 kN) for vertical and lateral loads, respectively. Lateral rail head displacements ranged between -0.05 to 0.16 inches (-1.27 to 4.06 mm) while dynamic lateral stiffness ranged from 42 to 62 kip/in. (7.3 to 10.8 kN/mm), indicating a low stiffness ratio for the DF fastener studied. Differences in behavior are attributed to dynamic vehicle-track interaction, the relationship between balanced and operating speeds, and differences in track gauge between sites. A comparison of vertical loading results with two additional heavy rail transit agencies shows Burr distributions that accurately represent the loading demands. Results from this study provide quantitative information that can be leveraged to improve heavy rail transit DF fastening system design and development of representative design validation testing protocols.

Keywords

Rail transit, direct fixation, slab track, loading environment, rail displacements, fastener stiffness

Date received: 29 July 2020; accepted: 16 December 2020

Introduction

More than half of all North American commuting trips within metropolitan areas are made on rail transit systems constructed before 1975; referred to as “legacy” systems.¹ Legacy systems face the challenge of maintaining aging infrastructure that is nearing the end of its life cycle, due in part to deferred maintenance with as much as 35% of US rail transit’s fixed guideway infrastructure considered to be in poor condition.² A large portion of rail transit’s infrastructure investment includes the track structure and its track fastening systems. Direct fixation (DF) fastening systems, one of the most common types of track systems used in US legacy heavy rail transit systems, are one component nearing the end of their service lives.

Direct fixation fastener use in the United States dates back to the 1960s, when they were installed on the New York Subway. Despite many advances in

design since their introduction, premature failures are still observed in newer DF systems, resulting in service disruption and increased maintenance expenditures. It is difficult to ascertain the exact cause of failures due to the complexity of loading conditions

¹Rail Transportation and Engineering Center – RailTEC, Department of Civil and Environmental Engineering – University of Illinois at Urbana-Champaign, Urbana, USA

²HDR Inc., Chicago, USA

³Department of Civil and Environmental Engineering – The University of South Carolina, Columbia, USA

Corresponding author:

Arthur de O Lima, Rail Transportation and Engineering Center – RailTEC, Department of Civil and Environmental Engineering – University of Illinois at Urbana-Champaign, 205 N. Mathews Ave., Urbana, IL 61801 USA.
Email: aolima@illinois.edu

and transfer of stresses within different track components under a variety of loads, track geometry characteristics, and environmental conditions. Factors influencing the behavior of DF fasteners, both internal and external, must be considered to better quantify their expected performance.

Most US rail transit agencies rely on consultants to develop technical documents and specifications regarding new component design and procurement. For DF fasteners, design specifications often mirror Transit Cooperative Research Program (TCRP) Report 71,³ with minimal modifications to adjust to a specific transit agency's operating conditions. Beyond TCRP 71, there is limited guidance that would facilitate optimized designs for any given rolling stock and operating conditions. Exceptions include light rail transit design guidance in the Track Design Handbook for Light Rail Transit⁴ and the limited guidance on DF track design in the American Railway Engineering and Maintenance-of-way Association's (AREMA) Manual for Railway Engineering.⁵ AREMA provides generalized static AW0 (i.e., empty) and AW3 (i.e., crush) loads quantified in previous research.⁶ While helpful, these values do not represent revenue service demands imparted on individual components, and requires load factoring to estimate dynamic demands on DF components.

Previous rail transit infrastructure research quantifying revenue service loading demands show differences in loading across modes.⁶⁻¹² However, no prior research focused specifically on heavy rail transit DF fastener performance, developed a comprehensive understanding of the revenue service demands, or identified mechanisms causing premature component failures.

This paper presents track loading demands and DF fastener response obtained through revenue service track instrumentation and is part of a broader research effort undertaken at a major US heavy rail transit property (hereafter referred to as the "agency") to provide insight into DF fastener design, behavior, and expected long-term fatigue performance by way of field, laboratory and numerical investigations. The agency has seen widespread premature failures of DF fastener assemblies (e.g., cracked plate or frame) and concrete structures (e.g., grout pad, invert, etc.).

Site location and DF fastener details

To investigate the effects of different operating conditions (e.g., track geometry, rolling stock vintage, etc.) three locations with DF track were instrumented. Field sites were located on curves with the same type of DF fastening system and were selected by the agency in consultation with the authors. Key characteristics considered for site selection were curve radius and the degree to which field failures had been

historically observed. No top-of-rail friction management or gauge-face lubrication were present at any of the sites. Evidence of minimal rail wear and high-rail flange contact were observed at all sites, but no signs of rail corrugation were noted. All sites were located far enough from station platforms to ensure trains maintained constant speeds through the site (i.e., no braking or acceleration).

The DF fasteners used by the agency at all three locations were a one-piece sandwich-type vulcanized bonded elastomer design with an elastic e-Clip and installed at 30-inch (76.2-cm) spacing with a threaded rod invert connection system. Additional details of each site location instrumented as well as the DF components are presented in Table 1.

Instrumentation overview

To quantify both loading demands and DF fastener response, multiple sensors were deployed at each site. Weldable strain gauges wired into Wheatstone bridges were installed on the web and base of the rail to quantify wheel-rail loading from revenue service trains using a proven methodology extensively deployed in the rail industry.^{8,9,13,14} Each bridge was calibrated by applying a known load to the rail and correlating loads to the measured voltage. Linear potentiometers were deployed using custom fixtures to capture rail head and base displacements as shown in Figure 1.

Data were recorded with a sampling rate of 2,000 Hz, a rate deemed adequate for the data collection of dynamic loads based on prior experiences.^{9,10,15} Data collection was performed at each site during weekday morning peak-service operations between 7:30 AM and 11:00 AM local time. On average, 70 train passes were recorded at each location for a total of 225 trains (or 14,830 wheels).

Results

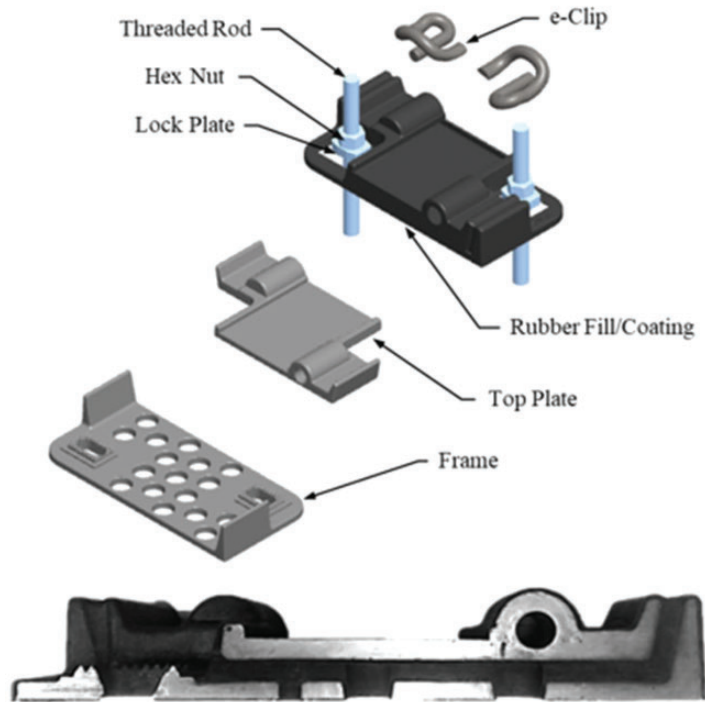
Load and displacement data are presented in the subsequent sections. Average train speeds were calculated for each train pass using the time between vertical load peaks and the known rolling stock axle spacing. Observed speeds ranged between 11.2 and 29.0 mph (17.9 and 46.4 km/h) with average of 24.0 mph (38.4 km/h) at Site 1, between 10.6 and 32.2 mph (17.0 to 51.5 km/h) with average of 24.4 mph (39.0 km/h) at Site 2, and between 18.7 to 39.0 mph (29.9 to 62.4 km/h) with average of 31.0 mph (49.6 km/h) at Site 3.

Vertical loads

Vertical load results are presented in Figure 2 as a percent exceeding graph. The most demanding loading conditions occur at Site 2, for both high and low rails, followed by Sites 1 and 3, respectively. At the

Table 1. General details of instrumentation sites and DF fastening system components.

		Site 1	Site 2	Site 3
Service Lines		A, B, C	A, B, C	D
Curve Radius	ft. (m)	769 (234)	755 (230)	1,200 (366)
Degree of Curve	°	7.44	7.59	4.77
Maximum Allowable Speed	mph (km/h)	35 (56)	40 (64)	50 (80)
Balanced Speed	mph (km/h)	24 (39)	27 (43)	36 (58)
Actual Superelevation (E_a)	in. (cm)	3.00 (7.62)	4.00 (10.16)	4.00 (10.16)
Unbalanced Superelevation (E_u)	in. (cm)	3.38 (8.59)	4.50 (11.43)	4.36 (11.07)
Design Gauge	in. (cm)	56.25 (142.88)	56.25 (142.88)	56.25 (142.88)
Measured Gauge	in. (cm)	57.00 (144.78)	56.50 (143.51)	57.00 (144.78)
Track Component Failure Rate		High	Low	High
Direct Fixation Fastener				
Components and Cross section				



extremes of these distributions, the 99.5th percentile load magnitudes recorded were 15.6 kips (69.4 kN) for Site 1, 16.6 kips (73.8 kN) for Site 2, and 14.4 kips (64.1 kN) for Site 3. The data also indicate higher vertical loads on the high rail compared to the low rail. This would indicate trains are operating at speeds above the curve's balanced speed (Table 1). Although this is true at Site 1, it is not observed at Sites 2 and 3.

Given these differences, high and low rail vertical loads for all sites are plotted in Figure 3 against corresponding speeds. Given the expected curvilinear relationship between speed and balance of forces, second order polynomial regression curves are plotted. Results demonstrate an expected positive quadratic relationship between high rail load and speed for Sites 1 and 2, while a negative relationship is observed at the low rail. However, while the low rail presents similar behavior at Site 3, high rail trends are

minimally negative; opposite of the expected relationship observed at the other two sites. Although the cause for reversal of the relationship is not obvious, one possible cause may be the shallower curve (approximately half the radius of Sites 1 and 2).

To further investigate the observed vertical loading environment and allow for better estimation of expected loads for future designs, a statistical analysis was performed to evaluate the results obtained and develop generalized distribution functions best representing the observed results. The Kolmogorov-Smirnov (K-S) test was employed to test the null hypothesis that the data from each site are drawn from the same continuous distribution.¹⁶ Considering a significance level of 5% ($\alpha = 0.05$), the null hypothesis was rejected concluding that the data are not part of the same distribution.

Next, the commercially-available software package EasyFit was used to fit and test approximately 65

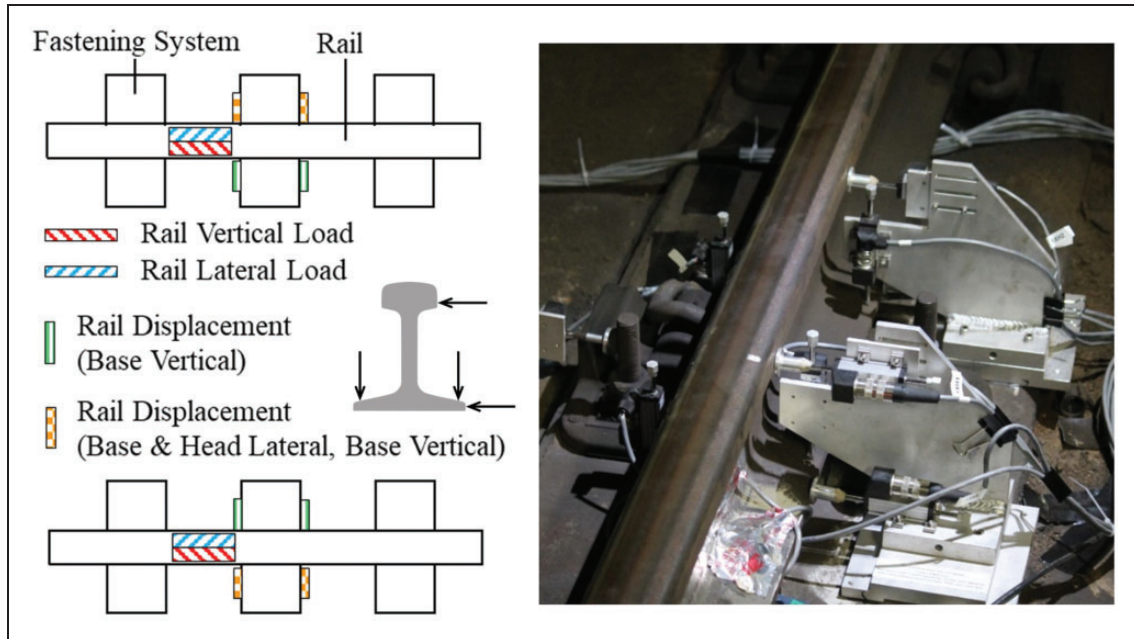


Figure 1. Plan view of field instrumentation layout (left); sensors and fixtures in the field (right).

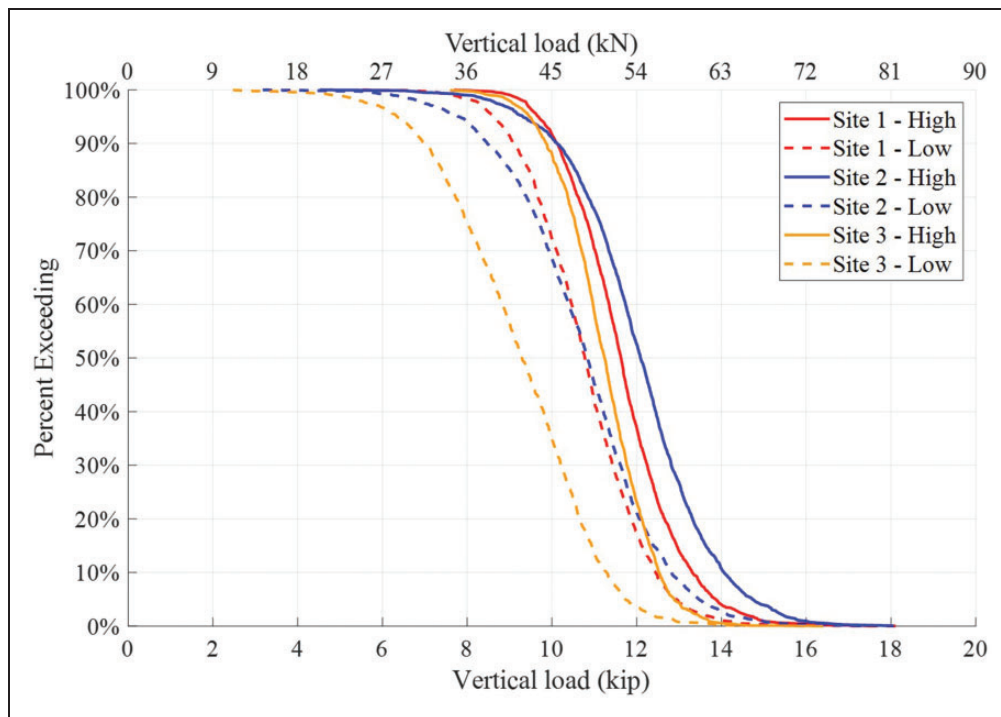


Figure 2. Measured vertical rail loads.

different types of typical distributions and evaluate their goodness-of-fit in order to determine the most appropriate for representing the sample dataset and develop a generalized probability distribution function (PDF).¹⁷ Goodness-of-fit was evaluated using the Anderson-Darling (A-D) test which is based on the K-S test but gives more weight to the tails of the distribution which are of key importance in this

analysis considering the relevance of extreme values for characterization of design load demands.¹⁸

Goodness-of-fit results concluded the Burr distribution to be the best fit for the data (Figure 4) and failed to reject the null hypothesis (i.e., that the data follow the specified distribution) for a significance level of 5% for Sites 1, 2, and the overall dataset, but not for Site 3. Given the results obtained from

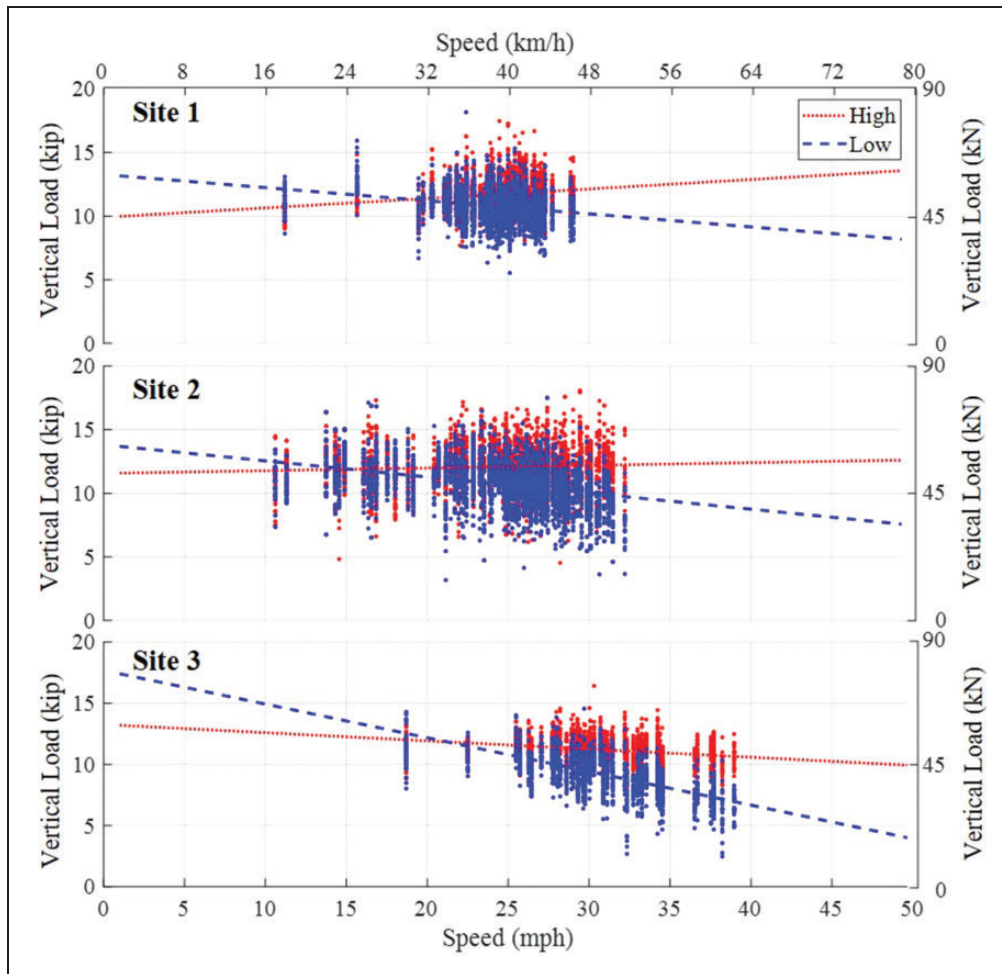


Figure 3. Relationship between speed and vertical load for high and low rails at all sites.

this analysis, the Burr distribution (equation (1)) was chosen to best represent the overall population of loads in the studied agency and the associated best fit cumulative distribution function is described by equation (2)

$$f(x) = 1 - \left(1 + \left(\frac{x - \gamma}{\beta} \right)^\alpha \right)^{-k} \quad (1)$$

$$f(x) = 1 - \left(1 + \left(\frac{x - 28.33}{40.20} \right)^{35.55} \right)^{-1.60} \quad (2)$$

Lateral loads

Lateral loads presented in Figure 5 indicate that Site 2 has the highest magnitude of lateral wheel-rail loads followed by Sites 3 and 1, respectively. In contrast to vertical loads, lateral loads on the low rail were generally larger compared to the high rail, except for the top 10% of loads at Site 1 and top 40% of loads at Site 3. The short radii of the sample curves indicate that wheels are likely not purely rolling, but creep is occurring and contributing to the low rail lateral

forces. Due to these short radii, track gauge plays an important role in the curving performance of the railcar's truck, and the resulting lateral loads imparted by each passing wheel. Track gauge values obtained from inspection car measurements taken around the time of instrumentation (Table 1) show that, on average, track gauge at Sites 1 and 3 was $\frac{3}{4}$ inch (1.9 cm) wider than design while the track gauge at Site 2 was only $\frac{1}{4}$ inch (0.6 cm) wider than design. This may be a contributing factor in the observed difference of lateral loading demands among the sites, especially between Sites 1 and 2 given their similar curve radii.¹⁹

There is a notable difference in behavior between leading and trailing axles of each truck, as evidenced by the difference in load responses of the top 50% (i.e., lead axles) from the bottom 50% (i.e., trailing axles) in Figure 5. This behavior is attributed to the rigid body curving of the trucks negotiating the curves and has been previously documented in heavy rail transit applications.^{11,20} Further, an analysis conducted to quantify the effect of vehicle type (i.e., vintages) on the loading demands found that Sites 1 and 2 average loads were independent of vehicle type. Site 3, however, presented larger lateral load demands for the newer rolling stock vehicles (with

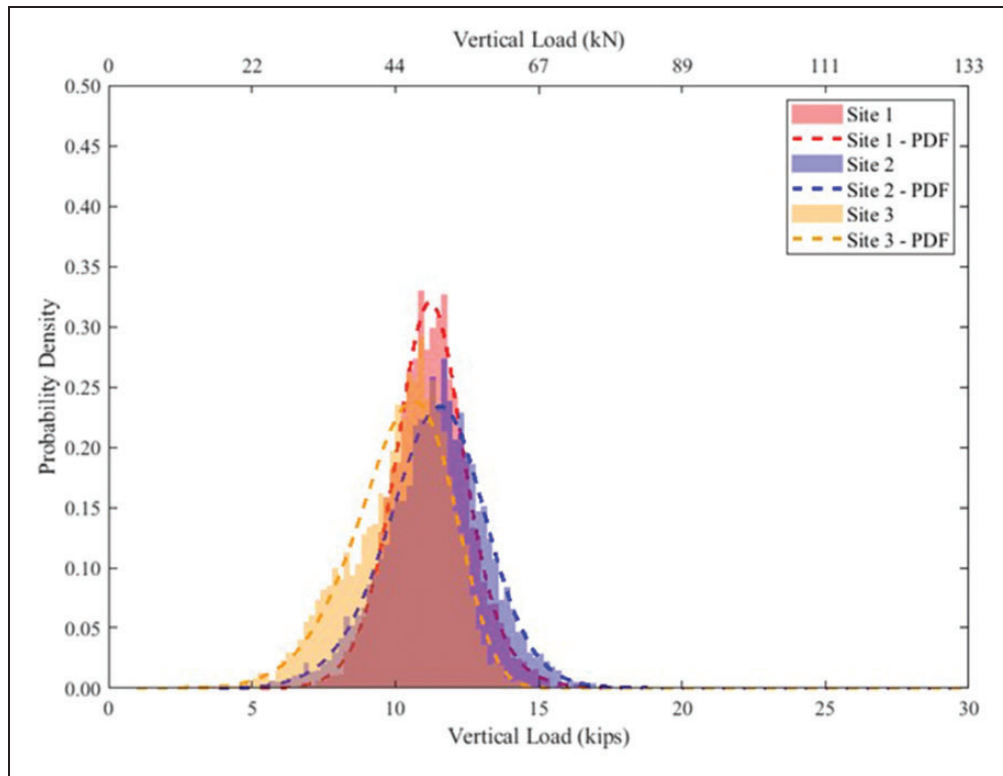


Figure 4. Vertical load histograms with associated probability distribution function (Burr).

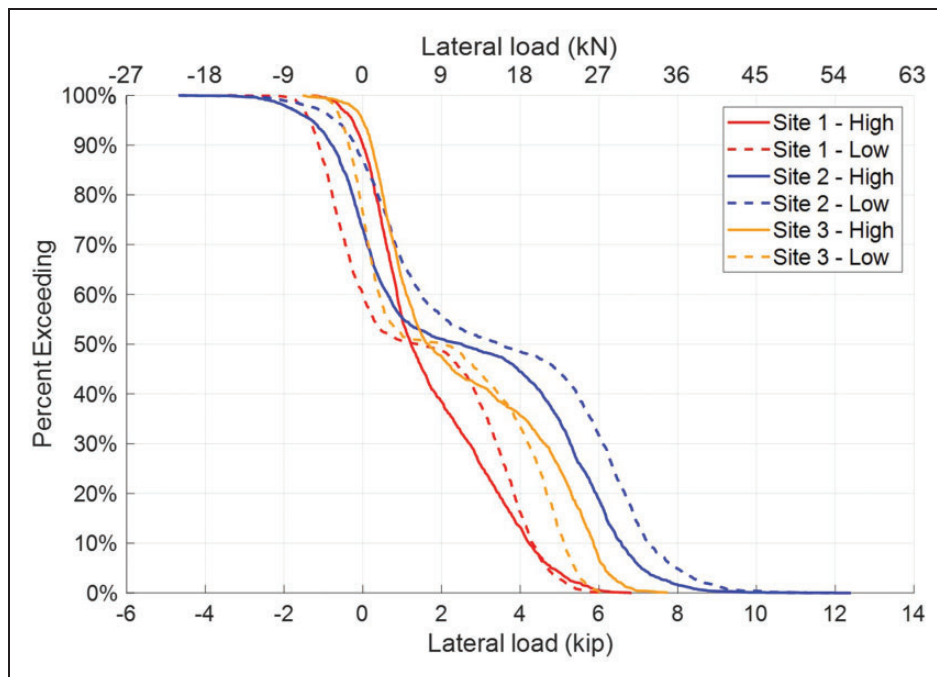


Figure 5. Measured lateral rail loads.

slightly higher wheel loads). Beyond a minimal difference in wheel loads, the difference in lateral loads could be related to differences in the truck curving behavior at Site 3 that may stem from effects of various conditions (e.g. curve radius, superelevation, gauge, etc.) either interacting or acting independently.

Rail displacements

Rail displacements provide valuable insight into the DF’s response to applied loads. Displacements are important given vertical and lateral stiffness are two critical design criteria specified for DF fasteners. Due to the large difference in observed lateral

behavior between leading and trailing axles, the analysis of lateral rail head displacements presented in Figure 6 considers only results from leading axles where positive rail displacement data indicates uplift or displacement towards the field.

Vertical displacements indicate rail rotation towards the field side in all rail seats, with the largest demands once again observed at Site 2. Although

lateral load results (Figure 5) show higher loads applied at the low rail, larger gauge side displacement is observed at the high rail, which is indicative of rotation magnitude. This may be related to the codependence of fastener displacements on both vertical and lateral forces (e.g., actions of vertical loads may cancel actions of lateral loads and vice versa).³

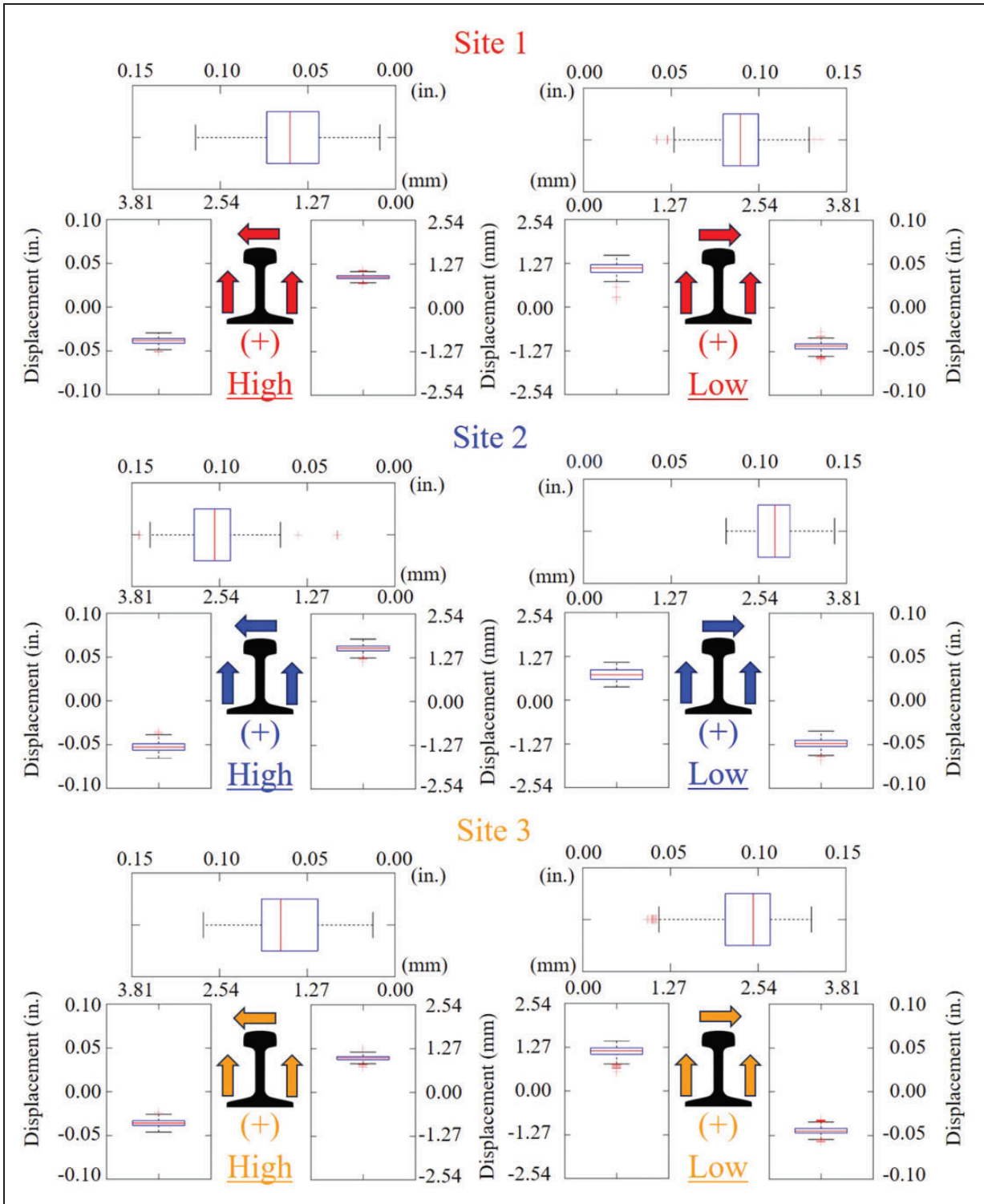


Figure 6. Measured vertical rail base and lateral rail head displacements.

Further, results in Figure 6 demonstrate the low rail experiences larger median rail head lateral displacements at all three sites. As was expected based on lateral loading results (Figure 5) and track gauge measurements (Table 1), the largest maximum and median displacements occurred at Site 2 for both high and low rails with median values of 0.10 and 0.11 inches (2.54 and 2.79 mm), respectively. The maximum gauge widening observed was 0.28 inches (7.11 mm), calculated by the summation of lateral rail head displacements at high and low rail under the same axle. While similar lateral displacements were observed between both rails in Site 2, median displacements were 0.03 inches (0.76 mm) greater on the low rail than the high rail at Sites 1 and 3 corresponding to a difference of 49% and 46%, respectively. As discussed, the short curve radii indicate creep is likely contributing to low rail displacements. Further, wheel flanging may also be a contributing factor to the observed outward rail head displacements.

While most of the data follows the expected behavior (i.e., increases in lateral load result in increases in lateral displacement) this is not the case at all sites. Site 3 was generally subjected to greater lateral loads on the high rail yet experienced larger lateral displacements on the low rail. It is hypothesized that this could be caused by the larger rail rotation constraints resulting from the higher vertical loads on the high rail at Site 3 as DF fastener lateral stiffness is dependent on vertical load.³

Fastener stiffness

As was previously mentioned, fastener vertical and lateral stiffnesses are key design parameters for DF systems. Due to the simultaneous presence of vertical and lateral loads over each fastener, and consequent rail rotation (Figure 6), it is not feasible to determine fastener vertical stiffness from the field data given it is difficult to differentiate between rail rotation and translation.

However, fastener dynamic lateral stiffness was estimated using linear least square regression models based on rail head displacements and corresponding lateral wheel loads (Figure 7). Given the non-linear stress-strain behavior of the DF elastomers,³ only leading axle values were included in the development of the regression model to determine fastener lateral stiffness.

While the average DF fastener dynamic lateral stiffness recorded was 53 kips/in (9.3 kN/mm), results from the six rail seats ranged from 42 to 62 kips/in (7.3 to 10.8 kN/mm) indicating variability in revenue-service dynamic stiffnesses. This is expected given the range of wheel loads, the dynamic loading environment, and the variability in behavior from the discrete rail supports.²¹ Nevertheless, stiffness results are within the range of values typically specified for

heavy rail operations (i.e., 30–64 kips/in (5.3–11.2 kN/mm)).^{3,4}

Consistent behavior was observed in Sites 1 and 3 with high R^2 values (all exceeding 0.8) while Site 2 presents greater variability with higher scatter and a lower R^2 . Contrary to historical failure rates (Table 1), several failed fasteners were observed in the curve that contained Site 2. Observed failures included cracked plates or frames, broken threaded rods, and/or cracked grout pads - although no individual DF fastener demonstrated a complete loss of performance. Failed fasteners could further influence train dynamics (e.g., variations in track lateral restraint generating hunting action), resulting in additional dynamic loads and displacements that generate variance in fastener response at the measurement site. These results, combined with the observed differences in track gauge, indicate there may be an acceleration of failure (i.e., negative feedback loop) where track dynamic behavior is affected by failed fasteners, leading to increased demands that further accelerate the deterioration of adjacent fasteners. This could also explain the difference between the historical rates of failure (Table 1) and the observed conditions and performance at each site (i.e., the historically low failure rate at Site 2 which demonstrated most demanding condition).

Although dynamic lateral stiffness results are on the high end of the specified range, this is expected given the intrinsic mechanical characteristics of elastomers (i.e., dynamic-to-static stiffness ratio) and the dynamic nature of the measurements taken. The influence of a high or low dynamic-to-static stiffness ratio to DF performance is not well understood. Most recommendations provide values between 1.3 and 2.0, indicating that static lateral stiffness for the DF fasteners studied could be as low as 21 kips/in (3.7 kN/mm).^{3–5} Beyond, these characteristics are important for other aspects of DF performance such as noise and vibration mitigation.^{4,22}

Discussion

This research quantified DF track wheel-rail loads and fastener displacement demands at several locations on a legacy heavy rail transit agency, demonstrating the variability of demands and responses within the same infrastructure type and operating environment. Several factors were identified as likely contributors to the variability: deviation between operating and balanced speeds, curve radius, track gauge, presence of failed fasteners, etc.

Therefore, data obtained in this study were compared to prior results from other rail transit systems to provide insight into the relative magnitude of the demands and responses observed. Table 2 presents a summary of loading values for two other legacy heavy rail agencies, a light rail transit agency, and a commuter rail operator.^{9,10} Data from all locations other

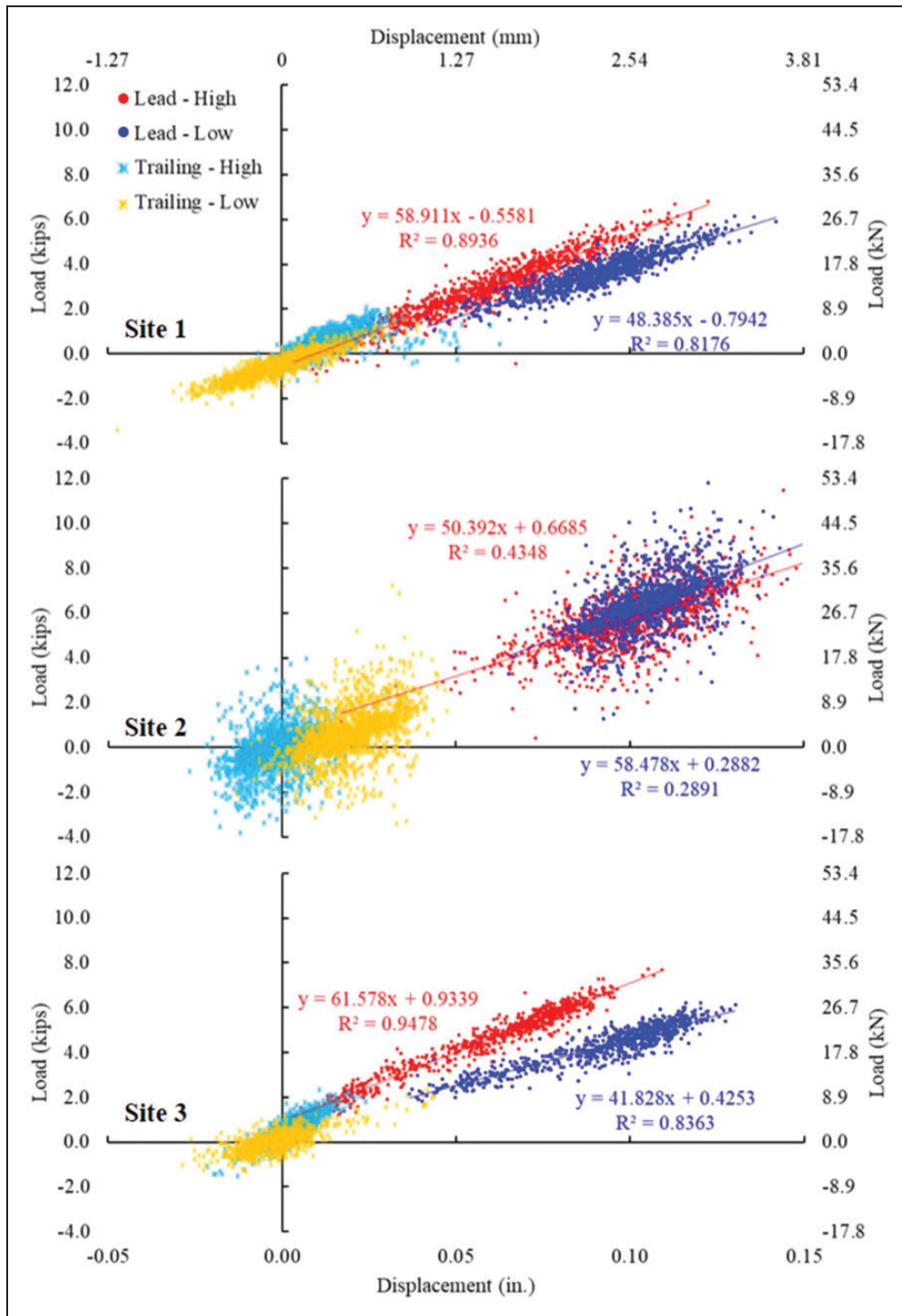


Figure 7. Fastener load-displacement scatter with linear model fit results for all sites.

Table 2. Vertical loading demands of various rail transit operators.

	Mean	95.0%	99.5%	Maximum
Heavy Rail 1 ^a	11.1 (49.4)	13.9 (61.8)	15.8 (70.3)	18.2 (81.0)
Heavy Rail 2 ^b	13.8 (61.4)	17.5 (77.8)	23.9 (106.3)	59.3 (263.8)
Heavy Rail 3 ^c	9.2 (40.9)	11.2 (49.8)	14.4 (64.1)	44.8 (199.3)
Light Rail ^d	8.1 (36.0)	9.8 (43.6)	11.2 (49.8)	18.6 (82.7)
Commuter ^e	18.1 (80.5)	30.7 (136.6)	38.0 (169.0)	41.1 (182.8)

Notes: All values in kips (kN).
 Results from - ^a14,830 wheels; ^b143,680 wheels; ^c1,955,712 wheels; ^d53,880 wheels; ^e338,742 wheels.

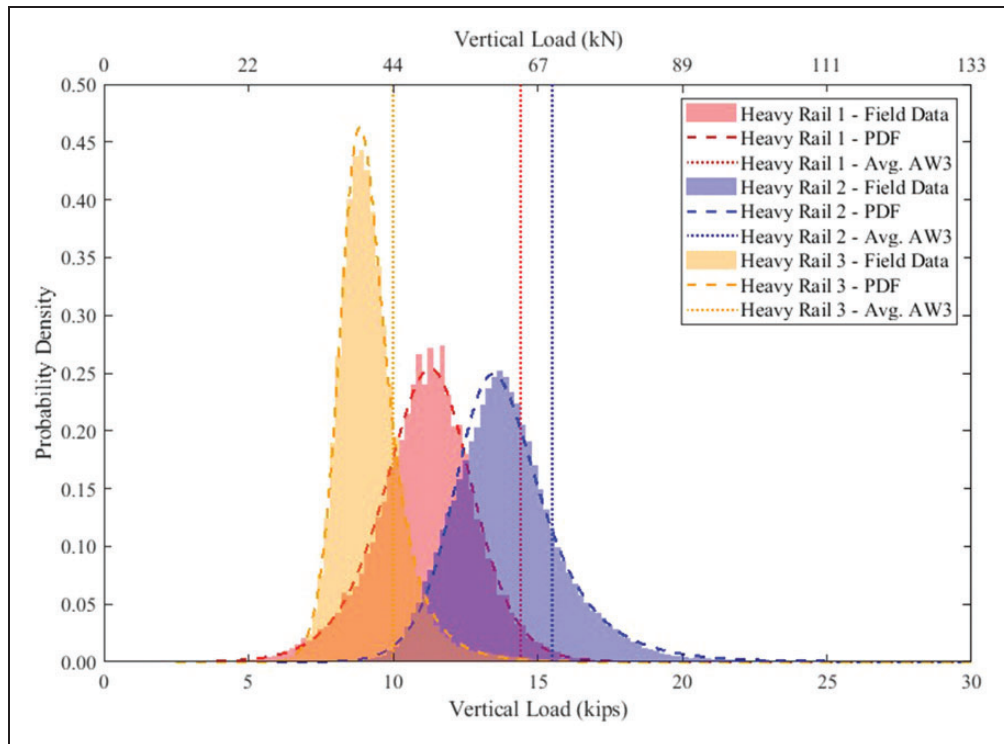


Figure 8. Vertical load histograms for three heavy rail agencies with associated probability distribution function (Burr) for measurements in curves (Heavy Rail 1 and 2) and tangent (Heavy Rail 3).

than the agency that is the primary focus of this paper (i.e., Heavy Rail 1) were obtained on ballasted track curves, and in tangent track for Heavy Rail 3.

The data demonstrate the variety of loading conditions across transit properties within the same mode (i.e., heavy transit) but even more significantly, across modes. These differences could result from the influence of agency-specific conditions including, track condition, operating practices, rolling stock type, rail/wheel profile, maintenance practices, etc. It is important, however, to consider the differences in sample size when comparing the results included in Table 2, especially when evaluating the tail of the distributions (i.e., data between 99.5% and Maximum). The relevance of a statistically sound data set for robustness of this comparison is evidenced by the capture of extreme values with larger sample sizes, likely related to impacts from out of round or flat wheels. Moreover, these findings indicate there may be a need to consider more demanding conditions when testing DF fasteners, especially in fatigue.³

Further investigating the specific demand conditions at heavy rail transit agencies, results from statistical analysis are compared to results from previous research.¹⁰ Results from K-S tests concluded all distributions (Figure 8) to be different while goodness-of-fit results from the A-D test failed to reject the null hypothesis and concluded that all data follow a Burr distribution ($\alpha = 0.05$).

The distributions presented in Figure 8 demonstrate the similarities between Heavy Rail 1 and 2 (both curved track locations), although the difference in distribution means is larger than the associated difference in the average AW3 loads between the agencies. This is likely attributed with differences in operating conditions (e.g., poorer wheel health), given AW3 loads are based on a fully loaded railcar. The longer and thicker tails of these distributions stem from the previously discussed curve balance and curving behavior of the rolling stock and contrasts the behavior observed for Heavy Rail 3, obtained from tangent track, which demonstrate a narrower distribution.

Given the results obtained from this analysis, Burr cumulative distribution functions (equation (1)) were also developed for the two additional heavy rail agencies (i.e. Heavy Rail 2 and 3) and are summarized below. Note that the cumulative distribution function representing Heavy Rail 1 is already presented in equation (2) and that for Heavy Rail 2 the coefficient gamma (γ) is zero.

Heavy Rail 2:

$$f(x) = 1 - \left(1 + \left(\frac{x}{13.27} \right)^{15.31} \right)^{-0.69} \quad (3)$$

Heavy Rail 3:

$$f(x) = 1 - \left(1 + \left(\frac{x - 3.61}{5.18} \right)^{11.07} \right)^{-0.70} \quad (4)$$

When evaluating the obtained distribution functions and comparing to current fatigue design load criteria presented in DF specifications, it is possible to observe that DF fatigue test loads could be refined to represent each agency's expected loading conditions. As an example, the maximum applied fatigue load for Heavy Rail 1 and 2 represent a 4.2% and 1.3% probability of occurrence, respectively, when using equations (2) and (3). For the latter agency, the maximum load is applied for 5% of the load cycles while a lower load, representing a 13.4% probability of occurrence, is applied during all other cycles.

Conclusions

The design and maintenance of DF track requires proper assessment of the revenue service demands and the resulting track responses. Currently, there is limited research to guide optimization of DF fastener designs for heavy rail transit. As such, this study included a focused field research effort aimed at improving the rail transit industry's understanding of such demands with the goal of providing a baseline for comparison of future DF track performance. Strain gauges and linear potentiometers were deployed to obtain rail loads and displacements. From the analysis and review of field data described within this paper, the following conclusions are drawn:

- Maximum revenue service vertical and lateral loads recorded were 18.2 and 12.4 kips (81.0 and 55.2 kN), respectively, both at Site 2
- Given similar curve radii and traffic conditions between Sites 1 and 2, the direct fixation fastening systems perform with an inherent level of variability
 - Variability likely stems from differences in track gauge, which was on average 1/2 in. (1.3 cm) narrower at Site 2
- Although average operating speeds were largely below balanced speeds, the high rail was consistently subjected to higher vertical loads than the low rail at all sites. In contrast, lower lateral loads were observed at the high rail in most cases, likely due to the curving behavior of the rigid trucks
- Vertical loads at all sites were found to follow similar shaped distributions, albeit statistically different
- Lateral rail head displacements ranged from -0.05 to 0.16 inches (-1.27 to 4.06 mm).
- In general, the low rail displaces more than the high rail, with differences ranging from -0.02 to 0.05 inches (-0.51 to 1.27 mm)
- Average dynamic lateral stiffness was 53 kips/in (9.3 kN/mm), and ranged from 42 to 62 kips/in (7.3 to 10.8 kN/mm), indicating a low stiffness ratio for the fastener studied
- The Burr distribution properly represents loading demands for all three heavy rail agencies studied

Results stemming from this study are relevant to the industry's understanding of how DF fasteners respond to the applied service loads while statistical distributions may be used to better estimate vertical loading demands. Finally, these data can be leveraged to improve heavy rail transit DF fastening system design and testing recommended practices.

Authors' contribution

The author's confirm contribution to the paper as follows: study conception and design: Luis Wally Chavez Quiroz, J. Riley Edwards and Yu Qian; data synthesis: Luis Wally Chavez Quiroz; analysis and interpretation of results: Luis Wally Chavez Quiroz, Arthur de O. Lima, J. Riley Edwards and Yu Qian; draft manuscript preparation: Arthur de O. Lima, Luis Wally Chavez Quiroz, J. Riley Edwards, Yu Qian, and Marcus S. Dersch. All authors reviewed the results and approved the final version of the manuscript.

Declaration of Conflicting Interests

The author(s) declared no potential conflicts of interest with respect to the research, authorship, and/or publication of this article.

Funding

The author(s) disclosed receipt of the following financial support for the research, authorship, and/or publication of this article: This research was funded in part by a US heavy rail transit property and by the National University Rail Center, a U.S. Department of Transportation Office of the Assistant Secretary for Research and Technology Tier 1 University Transportation Center. J. Riley Edwards has been supported in part by grants to the UIUC Rail Transportation and Engineering Center (RailTEC) from CN and Hanson Professional Services, Inc.

ORCID iDs

Arthur de O Lima  <https://orcid.org/0000-0002-9642-2931>

J Riley Edwards  <https://orcid.org/0000-0001-7112-0956>

Luis W Chavez Quiroz  <https://orcid.org/0000-0003-0475-833X>

Yu Qian  <https://orcid.org/0000-0001-8543-2774>

Marcus S Dersch  <https://orcid.org/0000-0001-9262-3480>

References

1. Cox W. *Transit Policy in an Era of the Shrinking Federal Dollar*. Report for The Heritage Foundation. Report no. 2763, 31 January 2013.

2. US Department of Transportation (US DOT). *2015 status of the nation's highways, bridges, and transit: conditions and performance*. USA: US Department of Transportation, 2015.
3. Transportation Research Board, National Academies of Sciences, Engineering, and Medicine. *Direct-fixation track design specifications, research, and related material*. Washington, DC: Transportation Research Board, 2005.
4. Parsons Brinckerhoff Inc., Metro Tech Consulting Services, Engineering and Architecture, P.C., et al. *Track design handbook for light rail transit*. 2nd ed. Washington, DC: Transportation Research Board.
5. AREMA. *Manual for railway engineering*. USA: American Railway Engineering and Maintenance-of-Way Association, 2012.
6. Lin X, Edwards JR, Dersch MS, et al. Load quantification of the wheel-rail interface of rail vehicles for the infrastructure of light rail, heavy rail, and commuter rail transit. *Proc IMechE, Part F: J Rail and Rapid Transit* 2018; 232: 596–605.
7. Canga Ruiz AE, Edwards JR, Qian Y, et al. Probabilistic framework for the assessment of the flexural design of concrete sleepers. *Proceedings of the Institution of Mechanical Engineers, Part F: Journal of Rail and Rapid Transit* 2020; 234: 691–701.
8. Edwards JR, Ruiz AEC, Cook AA, et al. Quantifying bending moments in rail-transit concrete sleepers. *J Transp Eng, Part A: Systems* 2018; 144: 04018003.
9. Edwards JR, Cook A, Dersch MS, et al. Quantification of rail transit wheel loads and development of improved dynamic and impact loading factors for design. *Proc IMechE, Part F: J Rail and Rapid Transit* 2018; 232: 2406–2417.
10. Edwards JR, de Lima AO, Dersch MS, et al. Resilient concrete crosstie and fastening system designs for light, heavy, and commuter rail transit. FTA Report No. 0158, Federal Transit Administration, <https://rosap.nhl.bts.gov/view/dot/44121> (accessed 1 February 2020).
11. Phillips C, Weinstock H, Greif R, et al. Measurement of wheel/rail forces at the Washington Metropolitan Area Transit Authority – volume I analysis report. DOT-TSC-UMTA-80-25, I, US Department of Transportation.
12. Phillips C, Weinstock H, Greif R, et al. Measurement of wheel/rail forces at the Washington Metropolitan Area Transit Authority – volume II test report. DOT-TSC-UMTA-80-25, II. US Department of Transportation.
13. Van Dyk, BJ, Edwards JR, Dersch MS, Ruppert Jr CJ., and Barkan CP. Evaluation of dynamic and impact wheel load factors and their application in design processes. *Proceedings of the Institution of Mechanical Engineers, Part F: Journal of Rail and Rapid Transit* 2017; 231(1): 33–43.
14. Harrison HD, Prause RH and Arnlund RC. Measurement plan for the characterization of the load environment for crossties and fasteners. FRA/ORD-77/03, Battelle Columbus Laboratories, April 1977.
15. Gao Z, Wolf HE, Dersch MS, et al. Field measurements and proposed analysis of concrete crosstie bending moments. In: *Proceedings of the American Railway Engineering and Maintenance-of-Way Association annual conference*, Orlando, FL, USA, 28-31 August 2016.
16. Sheskin D. *Handbook of parametric and nonparametric statistical procedures*. Boca Raton, FL: CRC Press, 1997.
17. MathWave Technologies. *EasyFit*. USA: MathWave Technologies, 2015.
18. Kvam PH and Vidakovic B. *Nonparametric statistics with applications to science and engineering*. Hoboken: Wiley & Sons, 2007.
19. Thompson D. *Railway noise and vibration: mechanisms, modelling and means of control*. Oxford UK: Elsevier, 2008.
20. Edwards JR, Dersch MS and Kernes RG. Improved concrete crosstie and fastening systems for US high speed passenger rail and joint corridors – project summary report (volume 1). Technical Report DOT/FRA/ORD-17/23, U.S. Department of Transportation, Federal Railroad Administration, Washington, DC, USA, November 2017.
21. Lu S, Arnold R, Farritor S, et al. On the relationship between load and deflection in the railroad track structure. In: *The 2008 Annual AREMA Conference*, Salt Lake City, UT, 21-24 September 2008, p. 2. Virginia Beach, VA: AREMA.
22. Hanson CE, Towers DA, Meister LTN, et al. Transit noise and vibration impact assessment. FTA-VA-90-1003-06, Harris Miller Miller & Hanson Inc., May 2006.